The Ionospheric Mapping and Geocoronal Experiment (IMAGER): a New System for Monitoring Ionospheric Space Weather

K. S. Wood
E. O. Hulburt Center for Space Research, Naval Research Laboratory

ABSTRACT

Ionospheric variability creates many practical problems that motivate efforts toward better forecasting and monitoring. At the same time it presents challenging plasma physics problems having to do with issues such as the development and propagation of irregularities. Ultraviolet remote sensing is among the best means of obtaining the required diagnostics to support both basic and applied research on these space weather effects. The methodology consists of measuring atomic and molecular lines of nitrogen and oxygen in the far- and extreme ultraviolet. By observing a complement of as few as four key lines it is possible to set up an effective monitoring system, providing practical parameters for ionospheric characterization as well as density profiles of relevant species. The global occurrence of ionospheric irregularities and the speeds with which they develop and propagate make it impractical to monitor them effectively from low earth orbit. The Ionospheric Mapping and Geocoronal Experiment (IMAGER) is a FUV/EUV imaging system for geosynchronous orbit now being constructed by the Naval Research Laboratory. The instrument consists of a telescope, filter system, and detectors that will obtain images of a 1000 km square field with 10 km resolution in a suite of spectral lines (1304, 1356, 1430 and 834 Å); it is able to provide diagnostics either on the day or night side, and either at nadir or on the earth limb. The GEO site for IMAGER and these instrumental capabilities will advance space weather monitoring toward the type of monitoring that has been achieved with satellite imagery for tropospheric weather. This work is sponsored by the Office of Naval Research.

1. INTRODUCTION

The Naval Research Laboratory is developing a new instrument for characterizing the Earth's thermosphere and ionosphere using ultraviolet remote sensing from geosynchronous orbit. This instrument will be used to study the spatial and temporal behavior of mesoscale (> 10 km) ionospheric structures, and is intended to be a step toward bringing monitoring of ionospheric irregularities to a level comparable to that available for tropospheric weather. The instrument is referred to by the name Ionospheric Mapping and Geocoronal Experiment (IMAGER). It was manifested for flight as a flyalong payload on another mission, but that mission was cancelled. During the interval when it was manifested it completed a formal Preliminary Design Review, then completed designs to a stage where flight procurements and assembly of an engineering model could begin. This paper describes the instrument concept, its history and development status, and its intended contributions to the study of space weather.

IMAGER observes naturally-occurring airglow with sensors that image in particular spectral lines. These sensors are passive in nature. With modern advances in multilayer filter design these sensors can be relatively compact. This instrument is designed to map and monitor the spatial and temporal evolution of mesoscale (> 10 km) structures in the thermosphere and ionosphere. It will observe the Earth's limb to derive daytime altitude profiles of O^+, O, O_2, and N_2 and will make nearly simultaneous observations of the edges of the northern and southern auroral ovals (on the sides toward the equator) to improve understanding of the energy deposition in these important atmospheric regions. The instrument consists of an extreme ultraviolet (EUV) imager and a far-ultraviolet (FUV) imager. The EUV imager will operate at 83.4 nm using a low resolution imaging spectrograph to set the passband. The O II 83.4 nm emission is produced by photoionization of O during the daytime. Above the limb, this emission can be used to determine altitude distribution of the O^+ density. The FUV imager will operate at 130.4 , 135.6, and 143.0 nm. At night, The O I 130.4 and O I 135.6 nm emissions are produced by primarily by radiative recombination, and therefore these emissions provide useful ionospheric diagnostics at night. During the daytime, the 130.4 and 135.6 nm lines are primarily produced by photoelectron impact excitation of O; however the 130.4 nm line is also excited by resonant scattering of sunlight. The O I 130.4 and 135.6 nm lines provide information on the O density during the daytime. The instrument will map the daytime N_2 column density using the Lyman-Birge-Hopfield bands near 143.0 nm.

IMAGER is designed to primarily operate at night because irregularities more likely during the evening, but it will also gather useful data on the day side of the earth. The instrument will be sensitive enough to gather a high signal-to-noise image viewing the nadir in approximately 100 seconds. The instrument can also be operated as a limb imager. The instrument will image a 1.6° degree field-of-view with 10 km spatial resolution. The imaged field of view nominally covers approximately 1000 x 1000 km, with exact values depending on the latitude and longitude at the center of the image. The instrument uses a two-axis gimbal to point to various points on the limb and disk of the Earth. The regions imaged are often pre-programmed, but other operational concepts including feedback from real time ground evaluation of the imagery are supported.

2. SCIENTIFIC PROGRAM

The experiment will attempt to answer several key science questions to improve our understanding of the coupled ionosphere thermosphere system. Its principal advance over earlier ultraviolet sensing of the ionosphere will come from being able to observe features and irregularities continuously as they evolve, rather than taking single images, as well as from being able to do this over the large fraction of the Earth visible to a single platform in geosynchronous orbit . The experiment will have ~10 km spatial resolution, ~100 s, high temporal resolution and high sensitivity (~500 ct/s/Rayleigh). These characteristics make it an ideal platform for specific science questions described below.

Key Science Questions

What is the global response of the ionosphere and thermosphere to solar and geomagnetic forcing? Many experiments have tried and others are trying to answer this question. This experiment will produce data looking at specified regions at different local times. The instruments can be trained on a particular region while observing changes in the structure of the ionosphere and thermosphere over that region at high (~100 second) time cadence. While ground-based instruments can make regional measurements, they are limited to studying regions above the places where they are deployed. For example, a single ground-based camera observing in a spectral line in the visible portion of the spectrum can track irregularities over a region comparable to the IMAGER field of view but cannot look at other regions nor can it follow the irregularity if it propagates out of that region. Also, observations can be done only at night and in clear weather. The latter point is potentially a limitation for exploring connections to lower altitudes, discussed below.

How are ionospheric composition changes related to the underlying neutral thermosphere? The ionosphere is produced by photoioization of O. One of the principal recombination loss processes is charge exchange of the O^+ with either N_2 or O_2 to produce N_2^+ or O_2^+. These species rapidly recombine with ambient electrons. The charge exchange process is strongly dependent on the N_2 and O_2 densities. The ratio of O to N_2 column densities has been observed to change during high geomagnetic activity. As this ratio decreases, the rate of photoionization of O decreases and the rate of recombination increases. Thus, the ionospheric electron density is expected to decrease because the production rate decreases and the loss rate increases. This has been observed using the *Dynamics Explorer* (DE) satellite (*Strickland et al.,* 2001). The DE data however, do not have very high spatial resolution and the temporal resolution is not very high due to the high degree of averaging of the data required to get high signal-to-noise. The experiment will be able to perform studies like the DE studies at temporal resolution of approximately 300 seconds (3 images at 100 seconds each) and at a spatial resolution of 10 km over a 1000 km field-of-view.

What are the characteristics, behavior, and origin of ionospheric bubbles and recently-observed mid-latitude depletions? The mid-latitude nighttime ionosphere has long been thought to have little morphological structure with only weak density gradients. However, recent measurements, including some with ground-based cameras, of the ionosphere at mid-latitudes at night have shown that strong mid- to small-scale ionospheric irregularities exist. The disturbances at mid latitudes generally propagate in a westerly direction, in contrast to those in equatorial regions. Figure 2 shows a frame from such an observation. The disturbances have complex shapes that evolve as they propagate.

How do the ionosphere and thermosphere respond to tropospheric influences? Recent theoretical calculations have indicated that the troposphere and stratosphere can perturb the ionosphere and thermosphere. The low- and mid-latitude ionospheric irregularity structures require a seed perturbation to initiate the instability. These perturbations may be induced by winds, gravity waves, or electric fields. Gravity waves may be induced by tropospheric dynamics. The effects of large tropospheric storms on the ionosphere and thermosphere cannot be observed from the ground, as the storm precludes gathering data. This is not a problem from space. This experiment will be able to look for ionospheric and thermospheric perturbations caused by tropospheric weather, obtaining the tropospheric information from some other source.

Daytime Observables

The complement of four spectral lines has been selected to provide a set of useful diagnostics for the distribution of ionization (electron content) and for densities of atmospheric species at nadir and limb, day and night. Moreover it will be seen in subsequent sections how the range of radiances encountered in these lines is to be covered with a single instrument observing from geosynchronous orbit.

The principal ionospheric observable during the daytime will be the O II 83.4 nm lines. The O II 83.4 nm emission is produced mainly by photoionization excitation of O at altitudes below 150 km. The 83.4 nm photons emitted downward are absorbed by the atmosphere. Those photons emitted upward enter the F-region ionosphere (altitudes 200 –600 km) where they undergo multiple resonant scattering by F-region O^+ ions. During the scattering process, the photons are entrapped and radiance field picks up a signature that depends on the altitude distribution of the O^+ ions. IMAGER will primarily use the 83.4 nm emission to characterize the ionosphere at the Earth's limb.

The experiment will observe the O I 135.6 nm and O I 130.4 nm emissions from neutral oxygen to infer the O density. On the dayside, both emissions are primarily excited by photoelectron impact. However, both show contributions from radiative recombination and O^+ – O^- mutual neutralization. The O I 130.4 nm emission is also excited by fluorescent scattering of sunlight at 130.4 nm.

The N_2 density will be inferred from measurements of the N_2 Lyman-Birge-Hopfield (LBH) band radiance. The N_2 LBH emission is excited by photoelectron impact. The experiment will observe the bands near 140.3 nm, as they are well separated from the O I 135.6 nm emission and the N I 149.3 emission. The 140.3 nm bands are also near the peak of the O_2 Shumann-Runge continuum (*Meier,*1991), which will allow the retrieval of the O_2 density by inversion of the limb measurements.

Nighttime Observables

The instrument will observe both the O I 130.4 and O I 135.6 nm emissions at night. These are excited primarily by radiative recombination of O^+ and electrons. A weaker component comes from O^+ – O^- neutralization. The O^+ and therefore the electron density (by charge neutrality) can be inferred by inversions of the nighttime radiance. *McCoy and Anderson* (1984) also demonstrated that the ratio of the O I 135.6 to O I 130.4 radiances could be used to infer the height of the ionosphere.

Radiances

IMAGER has been sized fro estimates of the radiances that will be encountered in the diagnostic spectral lines, merging information from previous instruments withtheoretical understanding and modeling. The lowest expected radiances provide overall sizing and other basic design drivers, while peak radiances determine performance characteristics for neutral density filters and contrast performance, that is, the edge response function.

Nighttime: Peak radiances were estimated by running the *International Reference Ionosphere* (IRI-90: *Bilitza*, 1990) for solar minimum and solar maximum conditions. Figure 1 shows a global map of the mid-solar cycle (10.7 cm solar flux of 140 solar flux units) peak electron density from the IRI-90. The radiances were then calculated by squaring the electron densities from IRI-90 and performing the line-of-sight integrations. The result was then scaled by the radiative recombination rate coefficients taken from *Melendez-Alvira et al.* [1999] and converted to units of Rayleighs. The limb radiances were derived from the nadir radiances by scaling them upward by a factor of 20 to account for limb brightening. The expected nadir radiances are: O II 83.4 nm less than 10 R, O I 130.4 nm between 0.1 R and 300 R (peak electron density 1×10^5 – 5×10^6 cm^{-3}), and O I 135.6 nm between 0.1 R and 300 R (peak electron density 1×10^5 – 5×10^6 cm^{-3}). The expected limb radiances are: O II 83.4 nm less than 10 R, O I 130.4 nm between 0.1 R and 3 kR, and O I 135.6 nm between 0.1 R and 3 kR. Although the N_2 LBH and O II 83.4 nm emissions are excited by sunlight so the nighttime radiances are expected to be nearly zero, some O II 83.4 nm emission has been observed at night (*Chakrabarti et al.,* 1984). This emission is thought to be scattered over from the dayside by O^+ ions in the magnetosphere.

Daytime: The nadir radiances were taken from *Meier* [1991]. The limb radiances were derived from these nadir radiances by scaling them upward by approximately a factor of 20 to account for limb brightening of the optically thin O I 135.6 and N_2 LBH 143.0 nm emissions. The O I 130.4 and O II 83.4 nm emissions are both optically thick and were instead scaled upward by approximately a factor of 2 to account for limb brightening. The expected limb radiances are: O II 83.4 nm between 1 R and 2 kR, O I 130.4 nm between 100 R and 20 kR, O I 135.6 nm between 1 R and 20 kR, and N_2 LBH 143 nm between 1 R and 1 kR. The expected nadir radiances are: O II 83.4 nm between 1 R and 1 kR, O I 130.4 nm between 100 R and 10 kR, O I 135.6 nm between 1 R and 1 kR, and N_2 LBH 143 nm between 1R and 100 R.

3. INSTRUMENT DESCRIPTION

The IMAGER design was driven by three basic requirements. First, the integration time to gather an image was selected to be 100 seconds, which is essentially a reflection of feature sizes and velocities of ionospheric irregularities as currently understood, with some allowance for future discovery. The experiment has a mode where it is expected to operate in near real time to provide ionospheric specification (at night) over a 1000 km region. Second, IMAGER must provide precise ionospheric specification, with 3 σ or better statistical uncertainty, over 100 km areas for the nighttime mid-latitude ionosphere. The minimum radiance assumed for the mid-latitude ionosphere was 0.1 Rayleigh. Third, the instrument is required to have 10 km spatial resolution to be able to resolve the structure of mid– and low–latitude ionospheric irregularities, as shown in Figure 2. These show spatial structures from the sub–kilometer level upward to the several thousands of kilometers. Equatorial irregularities propagate Eastward at approximately 10–100 meters per second, while mid-latitude irregularities, in contrast, propagate southwesterly at 10–100 meters per second. (Understanding this difference in propagation direction is an open research question at this time.) The electron densities, and therefore radiances, vary from levels present in the unperturbed ionosphere to nearly zero inside the depleted regions. Because optical properties of reflective materials vary substantially over the 83.4 nm – 143 nm wavelength range, the optical system had to be designed carefully with attention to the line radiances and the reflectivities of surfaces, to ensure requirements are met at all frequencies. The optical system consists of an off–axis parabolic telescope, which feeds an off–axis parabolic secondary mirror in a Gregorian telescope design (See Figure 5). The telescope has a 64 cm focal length and 16 cm aperture. The mirror surfaces have a magnesium fluoride over aluminum coating on zerodur blanks.

Although the FUV (longer than 120 nm) and EUV (83.4 nm) systems share common optics, they have different detectors and filter systems. For the EUV the single filter (83.4 nm) is built into the detector window, whereas for the FUV any of the three lines may be selected by rotating the appropriate filter into the optical path using a filter wheel. A fourth stop in the filter wheel has an open aperture so that when it is selected light passes through to the EUV instrument. The external and internal views of IMAGER are shown in Figures 4 and 5. Next, the FUV and EUV systems will be described individually.

Far–Ultraviolet System: After leaving the second reflector, light for the FUV system passes through a three–reflection narrow passband filter and onto another off–axis parabolic mirror (camera mirror) where it is imaged onto an imaging microchannel plate detector. The detector is a sealed tube type with a cesium–iodide photocathode. The detector readout is a delay line anode type, in two orthogonal directions. The filters are the three reflection bandpass filters developed for and flown on the Ultraviolet Imager (UVI) on the NASA *POLAR* satellite (*Zuckic et al.,* 1993). These filters have approximately 2.5 nm passbands (FWHM) and peak reflectances of 30–50%. Figure 5 shows the internal layout of the FUV imager.

Extreme–Ultraviolet System: The EUV system is active when the open aperture in the filter wheel is selected to be i n the optical path, so that, after leaving the second parabolic reflector, light for the EUV system passes through and reaches the EUV detector system. The EUV window filter is designed to provide 8 nm spectral resolution (FWHM), as the nearest bright emission features are the N II 91.6 and O I 91.1 nm lines. The telescope mirror and grating blanks will both be zerodur.

Calibration Spectrometer: We plan to include a calibration spectrograph to monitor any degradation in filter performance during flight. This spectrograph will view the same field-of-view as the imagers. The detailed design of the spectrograph has not been completed at this time. However, to adequately characterize the filter performance, the spectrograph must cover the 120–180 nm passband at 0.6 nm spectral resolution. The spectrograph does not need to provide imaging capability, and therefore, it will probably use a photomultiplier tube and scanning grating.

Sensitivity: The IMAGER instrument's sensitivity is estimated for the baseline design described above, using the following formula:

$$S = \frac{10^6}{4\pi} R^2 TQA\Omega$$

where the reflectance of the mirrors, *R*, is 0.8; the quantum efficiency of the detector, *Q*, is 0.1 (*Siegmund et al.,* 1987); the filter transmittance, *T*, is 0.5; the area of the primary mirror, *A*, is 316 cm^2; the solid angle, Ω, is 8×10^{-4} steradians; and the constant $10^6/4\pi$ converts the results to Rayleighs. The resulting sensitivity at 135.6 nm is 320 counts per second per Rayleigh. This sensitivity is approximately the same for the N_2 LBH 143 and O I 130.4 nm passbands.
The resulting sensitivity for the EUV system at 83.4 nm is 1.3 counts per second per Rayleigh.

Signal-to-Noise Ratio: The signal–to–noise ratio for the sensitivities of the instrument from above combined with the minimum radiances from above are estimated assuming that there is negligible dark count (reasonable for microchannel plate detectors with cesium iodide photocathodes) and assuming 100 × 100 km superpixels (dividing the image into 10^2 superpixels by binning), plus an integration time of 100 seconds. The following formula was used:

$$N = S\Delta t I \Big/ \left(10^2\right)$$

where *S* is the sensitivity; Δt is the integration time (100 S); *I* is the minimum radiance; and 10^2 is the number of superpixels in the image. The results give signal to noise ratios that are all larger than the values established as observational requirements.

Gimbal: We intend to use a two–axis gimbal to point the instruments. This provides the minimum volume for the imagers, as the number of reflections are minimized. The gimbal is designed to slew from limb to limb, an angular travel of 25°, in 5 minutes. The Earth subtends approximately 17°, when viewed from geostationary orbit. The gimbal system must allow for a field-of-regard of 25° to allow for limb measurements and to allow stellar calibration. The gimbal must be able to point center of the instrument's field-of-view to a point on the globe to an accuracy of 50 km. The primary requirement for the gimbal system emphasizes pointing knowledge. The location of the center of the field-of-view must be known to an accuracy of 20 km to accomplish the mission's imaging objectives.

4. EVOLUTION OF MISSION CONCEPT

IMAGER has for several years been carried as a manifested flight payload under the U.S. Air Force Space Test Program (STP). Prior to that it had been favorably evaluated in experiment reviews conducted for STP, from which evaluation resulted efforts to find it a flight opportunity on some large satellite intended for geosynchronous orbit, in accordance with the standard procedures of the STP. IMAGER instrument was initially intended to fly on the *GIFTS/IOMI* mission, which was sponsored jointly by NASA, the U.S. Navy, and NOAA. Under this plan IMAGER would have flown alongside a large imaging Fourier Transform spectrometer, designed to image tropospheric and stratospheric weather in the optical to infrared portion of the spectrum. While both IMAGER and the Fourier Transform spectrometer may eventually fly, their flight on the same spacecraft is no longer particularly likely.

During the years 2001-2002 the joint mission was fully staffed and moving through a succession of design reviews preparatory to fabrication. Work under the *GIFTS/IOMI program* refined the IMAGER operations concept, to include both a nominal mode in which the sequence of operations is pre-programmed and an occasional mode in which downlinked images are rapidly processed and evaluated in real time, with subsequent uplink of commands either to change filters or the Earth region selected for observation. IMAGER instrument development kept pace with the *GIFTS/IOMI* schedule and included a complete design evaluation and redesign during 2001-2. There was considerable rework motivated by need to reach the weight and power targets for that mission. (These targets are regarded as likely to be representative of any subsequent mission.) The instrument description above refers to the end product of this effort, for which a Preliminary Design Review (PDR) was held in June, 2002. The PDR covered optical, mechanical and electrical design as well as a thorough review of science requirements, other requirements for support of studying related issues in operational monitoring of ionospheric weather, and flowdown of these requirements to the scientific design. Analysis showed, for example, that the design being fabricated was able to meet the contrast requirements that had been established for observing faint features near bright ones. Point response, line response, and edge response functions for the instrument were produced by simulation.

Design refinement continued after the PDR, but by now it was becoming clear that the *GIFTS / IOMI* mission was in some danger. The design was accordingly kept as generic as possible to facilitate attachment to a different geosynchronous satellite should that prove necessary. By the time of the *GIFTS/IOMI* cancellation (late 2002) many of the IMAGER designs were matured to where space hardware fabrication could commence. An Engineering Model, which is largely flight-qualified hardware, is being constructed in 2003-4.

5. ACKNOWLEDGMENTS

The Office of Naval Research funds the design and development of the IMAGER instrument. R. McCoy originally proposed the instrument and D. Prinz carried out the first optical design. Many individuals are now contributing to the IMAGER design. The Project Scientists are K. Dymond and S. Thonnard. The Mission Integration Scientist is M. Lovellette. P. Kalmanson has led the mechanical design and G. Clifford has led the electrical design. G. Fritz has requirements definition and vendor selection for the detectors. The new optical design has been done by J. Wilczynski and C. Ftaclas has contributed to the system analysis.

6. REFERENCES

Bilitza, D., *International Reference Ionosphere 1990*, National Space Science Data Center, NSSDC/WDC-A-R&S 90-20, Greenbelt, Maryland, 1990.

Chakrabarti, S., Kimble, R., and Bowyer, S., "Spectroscopy of the EUV (350–1400 Ä) Nightglow"*, Journal of Geophysical Research,* **89**, 5660, 1984.

McCoy, R. P., and D. E. Anderson, Jr., "Ultraviolet remote sensing of the F2 ionosphere", Effect of the Ionosphere on C3I Systems; Ionospheric Effects Symposium, 295-302, 1984.

Meier,R. R., "Ultraviolet Spectroscopy and Remote Sensing of the Upper Atmosphere", *Space Science Reviews*, **58**, No. 1 & 2, 1-186, 1991.

Melendez-Alvira, D. J., Meier, R. R., Picone, J. M., Feldman, P. D., and McLaughlin, B. M., Analysis of the Oxygen Nightglow Measured by the Hopkins Ultraviolet Telescope: Implications for Ionospheric Partial Radiative Recombination Rate Coefficients, *Journal of Geophysical Research*, **104**, 14901, 1999.

Siegmund, O. H. W., Everman, E., Vallerga, J. V., Sokolowski, J., and Lampton, M., "Ultraviolet Quantum Efficiency of Potassium Bromide as an Opaque Photocathode Applied to Microchannel Plates", *Appl. Optics*, **26**, No. 17, 1987.

Strickland, D. J., Craven, J. D., and Daniell, R. E., "Global Enhancements in O/N_2 Recorded by the DE-1 FUV Imager During Geomagnetically Disturbed Periods", *Eos Trans. AGU*, **84** (20), Spring Meeting Suppl., Abstract SA62A-02, 2001.

Zuckic, M., Torr, D. G., Kim, J., Spann, J. F., and Torr, M. R., "Filters for the International Solar Terrestrial Physics Mission Far-Ultraviolet Imager", *Optical Engineering*, **32,** 3069, 1993.

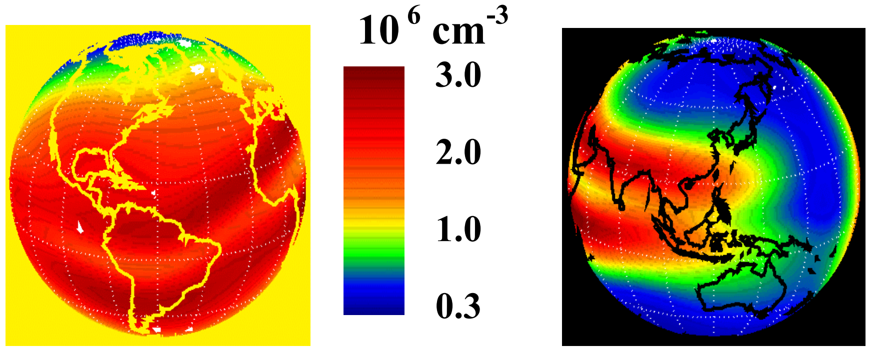

Figure 1: This figure shows a map of the peak F-region electron density for mid-solar cycle conditions (10.7 cm flux of 140 solar flux units) at vernal equinox. The peak density varies by an order of magnitude over the globe. The left hand panel is the daytime electron density while the right hand panel shows the nighttime electron density.

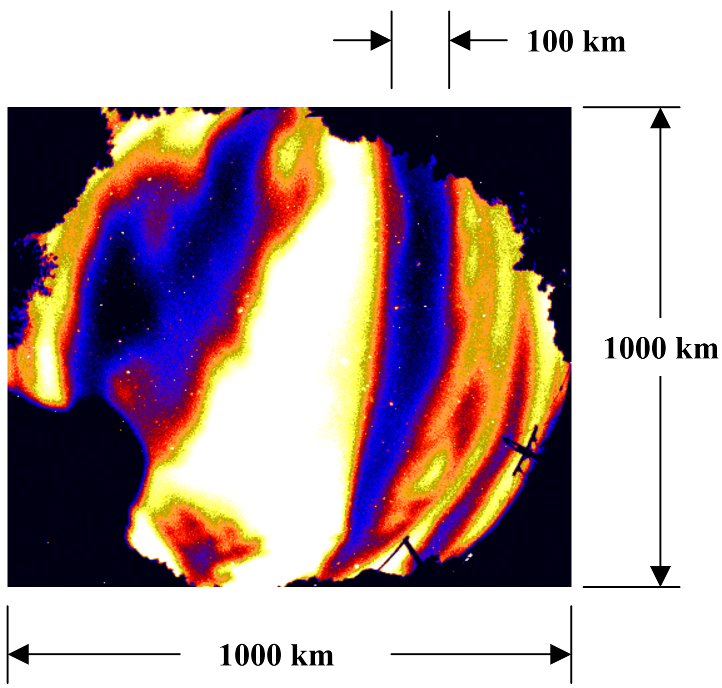

Figure 2.: This is an all sky camera image at 630 nm of a mid-latitude irregularity. This image was acquired at the Arecibo Incoherent Scatter Radar Facility in Puerto Rico by J. Makela (Cornell U.). The black irregular border is from near field objects, such as trees and telephone poles. The bright bands running across the image from top to bottom are the undisturbed ionosphere. The dark bands running from top to bottom are ionospheric depletions or irregularities. These irregulariteis propagate in a southwesterly direction at 10-100 m/s. The electron density in these regions is nearly zero.

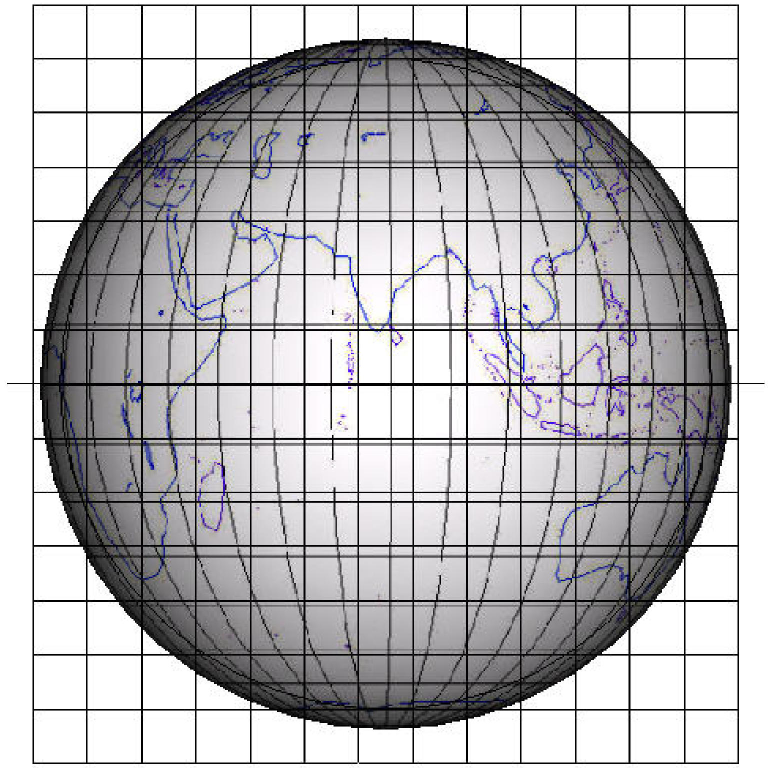

Figure 3.: The Earth as viewed by IMAGER from geosynchronous orbit. Each square in the image is 1000 × 1000 km.

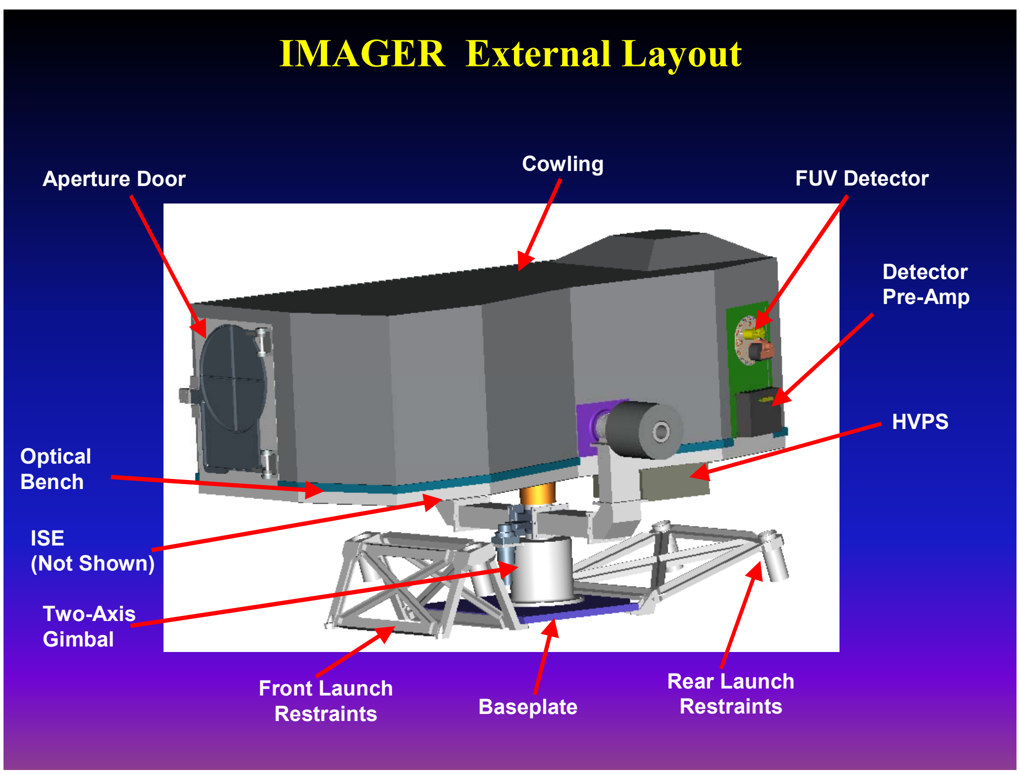

Figure 4.: This shows the external layout of the IMAGER payload.

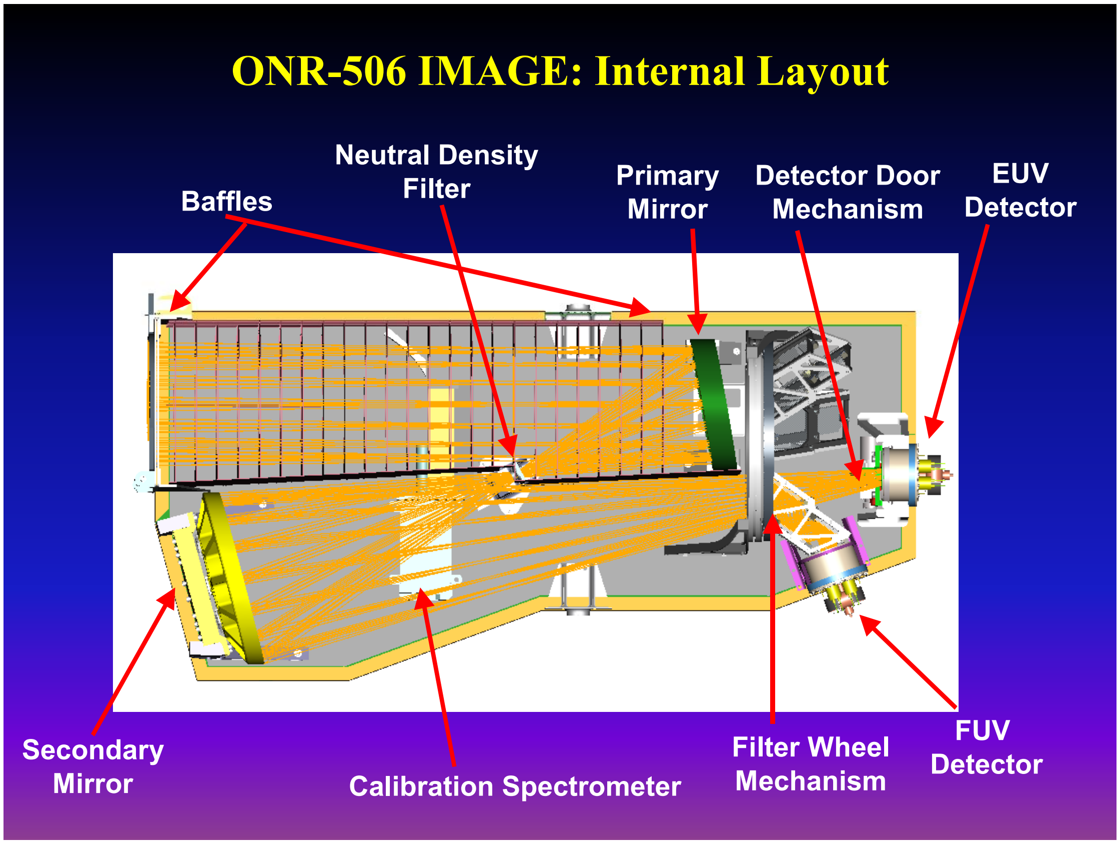

Figure 5.: This is a drawing of the internal layout. The Gregorian telescope design combined with the rotating filter wheel allows a single set of mirrors to serve both the FUV and EUV detectors. Each position of the filter wheel mechanism selects for a single observing frequency. The FUV filters deflect the accepted light to the FUV detector. An open position in the wheel, if selected, permits light to pass to the EUV detector, where the EUV filter (83.4 nm) is built into the entry window.